JOURNAL OF SPACECRAFT AND ROCKETS
Vol. 45, No. 6, November–December 2008

Projectile Aerodynamics Overtaking a Shock Wave

G. Rajesh* and H. D. Kim†
Andong National University, Andong 760-749, Republic of Korea
and
T. Setoguchi‡
Saga University, Saga 840-8502, Japan

DOI: 10.2514/1.35398

A projectile that passes through a moving shock wave experiences drastic changes in the aerodynamic forces as it moves from a high-pressure region to a low-pressure region. These sudden changes in the forces are attributed to the wave structures produced by the projectile–shock-wave interaction and are responsible for destabilizing the trajectory of the projectile, consequently leading to a loss of projectile stability and control efficiency. A computational study was performed here using a moving-grid method to analyze the effects of the projectile overtaking a moving shock wave on the projectile aerodynamic characteristics. A one-dimensional analysis was also carried out to identify the projectile overtaking criteria. The analytical results show that the projectile overtaking flowfields can be in a subsonic or supersonic flow regime, based on the relative projectile Mach number. However, it is found that the actual flowfields in the present computations cannot be distinguished with the relative projectile Mach number only, because the blast-wave strength is diminishing with time and space. The aerodynamic characteristics of the projectile are hardly affected by the overtaking process for smaller blast-wave Mach numbers, as the blast wave will become weak by the time it is overtaken by the projectile. The projectile drag coefficient is more greatly affected by the unsteady flow structures through which the projectile travels in the near field than by the overtaking process.

Nomenclature

A	=	area, m^2
a	=	speed of sound, m/s
C_d	=	drag coefficient
D	=	drag force, N
M	=	Mach number
M_{p1}	=	projectile Mach number relative to still air
M_{p2}	=	projectile Mach number relative to flow behind the moving shock wave
M_s	=	shock wave Mach number
p	=	pressure, N/m^2
T	=	temperature, K
t	=	time, ms
u	=	velocity, m/s
γ	=	ratio of specific heats
ρ	=	density, kg/m^3

Subscripts

p	=	projectile
s	=	shock wave
1, 2	=	downstream and upstream of the moving shock wave

I. Introduction

WHEN a projectile suddenly starts to move in the launch tube of a ballistic range, a series of compression waves are formed ahead of the projectile, due to its piston effect. These compression waves coalesce into a normal shock wave for which the strength depends on the acceleration of the projectile. The shock wave propagates toward the exit of the launch tube and is discharged from the launch tube, forming a spherical blast wave due to the shock diffraction at the exit of the launch tube. This blast wave is usually called the primary blast wave (PBW) and develops with associated starting vortices at the exit of the launch tube [1–3].

Shortly after the discharge of the shock wave from the launch tube, the compressed gas between the shock wave and moving projectile inside the launch tube is discharged. A contact surface is formed at the boundary of the compressed gas and the ambient gas that was perturbed earlier by the blast wave. Behind the contact surface, an unsteady jet is developed by the discharge of the compressed gas. This unsteady jet may often be accompanied by a shock wave, the strength of which is dependent on the projectile acceleration [4].

Following the unsteady jet, the projectile is discharged, consequently leading to strong interaction between the projectile and the unsteady jet when the former passes through the preceding unsteady jet. The effects of this interaction are usually reflected in the unsteady fluctuating forces that act on the projectile itself [5]. As the projectile moves forward, a bow shock wave may be produced in front of the projectile, depending on the projectile speed and local flow conditions. The projectile flowfield, being time-dependent, is influenced strongly by the preceding PBW and bow shock wave. As time advances, the projectile may or may not overtake the preceding PBW within a short distance, subject to certain conditions that will be discussed later, in more detail.

Meanwhile, the high-pressure gas that, in general, is obtained by the combustion explosion in the ballistic range [6] and used to drive the projectile initially is discharged immediately after the projectile is ejected from the launch tube. The secondary blast wave (SBW) is formed due to the sudden discharge of this high-pressure combustion gas. The so-called Ritchmyer–Meshcow instability develops when the contact surface following the PBW is swept by the SBW [7].

A highly underexpanded supersonic jet is produced due to the discharge of the high-pressure combustion gas. Inside the jet, a strong Mach disk is formed to match the pressure levels behind the moving projectile. If the discharged high-pressure combustion gas maintains a constant mass flow rate, the underexpanded jet structure will be steady [8]. The characteristics of this jet are quite different from that of the unsteady jet produced in front of the projectile by the

Received 15 December 2007; revision received 5 May 2008; accepted for publication 11 June 2008.

*Doctoral Student, School of Mechanical Engineering; rajesh@anuis.andong.ac.kr. Student Member AIAA.
†Professor, School of Mechanical Engineering; kimhd@andong.ac.kr. Member AIAA (Corresponding Author).
‡Professor, Department of Mechanical Engineering.

discharge of the compressed gas between the normal shock wave and the projectile during the early stages of projectile discharge. For a typical case of a projectile discharged from a launch tube [9], Fig. 1 shows all the associated flow structures, where t is the time lapsed from the instant of the projectile movement.

As already described, the flowfield around the moving projectile is highly complicated as well as strongly time-dependent. There are various types of interactions among the shear layers, shock waves, and wake flow behind the projectile and the moving projectile itself. These complex flow phenomena will be reflected in the aerodynamic forces acting on the projectile and thus strongly influence the flight control and stability of the projectile [10].

All of these coupled phenomena take place in a very short interval of time, and the measurement of the detailed aerodynamics is extremely difficult. So far, the investigation of the projectile aerodynamics and aeroballistics has been limited to the visualization of such flowfields using a high-speed optical system [11], and quantitative data associated with the flying projectile aerodynamics are sparse to date. It is expected that the aerodynamic forces drastically change as the projectile interacts with the unsteady jet and the shock systems around it, or it passes through the primary blast wave [12]. For example, as the projectile passes through the primary blast wave or the projectile interacts with the preceding unsteady jet, it experiences a sudden change in the aerodynamic drag.

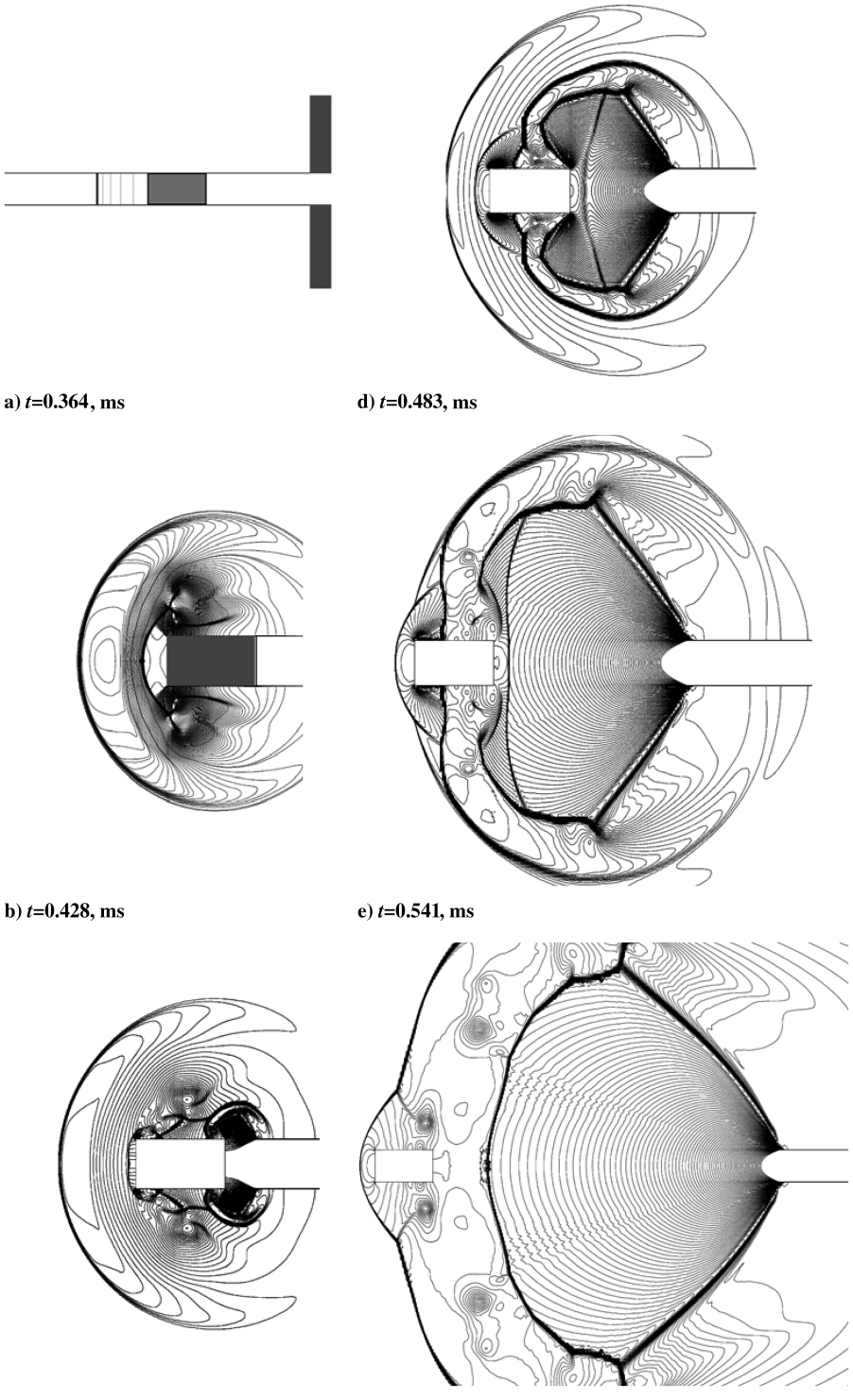

a) t**=0.364, ms** **d)** t**=0.483, ms**

b) t**=0.428, ms** **e)** t**=0.541, ms**

c) t**=0.435, ms** **f)** t**=0.716, ms**

Fig. 1 Flowfield associated with the discharge of a projectile from a launch tube [9].

The aerodynamic force data associated with such situations are highly lacking or have been ambiguously conjectured until now.

Only a few works [9–12] have been made to date to investigate such an interaction flowfield around the flying projectile. Thus, the prediction of the unsteady projectile aerodynamic data is now one of the extremely challenging works that are being paid much attention from researchers and aerodynamic designers.

Of many aspects of the unsteady projectile aerodynamics already described, one of the most important phenomena occurs as the projectile overtakes the preceding blast wave. Recently, Watanabe et al. [13] investigated the projectile overtaking flowfields to study the projectile aerodynamics. They used a one-dimensional analysis to study the overtaking criteria and argued that the overtaking process can be either subsonic or supersonic, based on the projectile Mach number relative to the flow behind the blast wave. They arbitrarily assumed the projectile and blast-wave Mach numbers and their computations started from a steady-state solution of the flowfield. The blast wave maintained constant strength throughout their computations. Later, Ahmadikia and Shirani [14] performed viscous computations on transonic and supersonic overtaking flowfields using similar assumptions. In both of these works, the relative projectile Mach number was the major factor to decide the overtaking criterion. However, in actual situations in which the blast-wave propagation is a transient phenomenon, the strength of the blast wave will be decreasing and the relative projectile Mach number will no longer be constant during the whole overtaking process. In such a situation, neither the flowfields nor the projectile aerodynamic characteristics can be determined accurately based on the relative projectile Mach number. Moreover, the transient structures of the flowfield will have a deterministic effect on the aerodynamic characteristics of the projectile.

Hence, in real situations in which the spherical blast wave is propagating, the overtaking process will be completely different from that of a steady blast wave with constant strength. The overtaking process being purely time-dependent, it is not known exactly at what conditions the projectile overtakes the blast wave and what parameters control the overtaking problem. Moreover, the collection of detailed projectile aerodynamic data at the instant when the projectile overtakes the blast wave is an exciting problem to the aerodynamic designers.

The present study aims at investigating the projectile overtaking aerodynamics and the detailed overtaking flowfield. One-dimensional analysis was performed to shed new lights on the overtaking flowfields. A computational fluid dynamics (CFD) method using a moving-grid system was employed to simulate the projectile aerodynamics on such flowfields. The present computations successfully capture the projectile aerodynamics characteristics and well predict the projectile acceleration, velocity, and aerodynamic drag, which were difficult to obtain in experiments.

II. One-Dimensional Analysis of the Projectile Overtaking

In general, the speed of sound downstream of a shock wave is higher than that upstream of it. Thus, a wave or an object can overtake the preceding shock wave, depending on the strength of the shock wave and the speed of the object relative to the flow behind the shock wave. To analyze the projectile overtaking problems, we assume the overtaking flow to be unsteady and one-dimensional. The primary blast wave is hence assumed as a normal shock wave with a constant propagation speed. For a given normal shock wave that propagates at a constant speed of Mach number M_s in still air, the flow properties can be calculated behind the shock wave. It is also assumed that a projectile with speed u_p is propagating toward the normal shock wave, as schematically shown in Fig. 2.

Assuming that the flow states across the shock wave are denoted by the subscripts 1 and 2 and the projectile velocity is given by u_p, the shock wave Mach number M_s and the projectile Mach number M_{p1} can be defined as

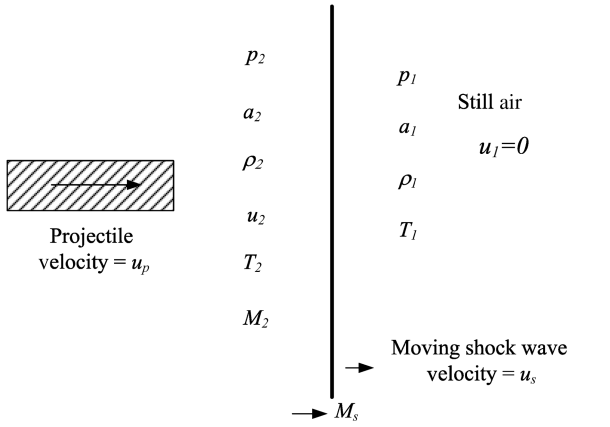

Fig. 2 Schematic diagram showing the projectile motion relative to the blast wave.

$$M_s = \frac{u_s}{a_1}, \qquad M_{p1} = \frac{u_p}{a_1} \tag{1}$$

The projectile Mach number M_{p2} relative to the flow state behind the moving shock wave is obtained by

$$M_{p2} = \frac{u_p - u_2}{a_2} \tag{2}$$

In Eq. (2), the projectile motion is supersonic relative to the flow state behind the shock wave if M_{p2} is larger than 1.0 and is subsonic if M_{p2} is less than 1.0, and Eq. (2) can be written as

$$M_{p2} = M_{p1}.\frac{a_1}{a_2} - M_2 \tag{3}$$

Hence, for the supersonic overtaking,

$$M_{p1} > (1 + M_2)\frac{a_2}{a_1} \tag{4}$$

and for subsonic overtaking,

$$M_{p1} < (1 + M_2)\frac{a_2}{a_1} \tag{5}$$

Using 1-D gas-dynamic equations for a moving shock wave, the Mach number M_2 and the speed of sound a_2 of the flow behind the shock wave can be expressed as a function of M_s, and Eq. (3) becomes

$$M_{p2} = \left\{ M_{p1} \Big/ \left[\left(1 + \frac{2\gamma}{\gamma+1}(M_s^2 - 1) \right) \left(\frac{2 + (\gamma-1)M_s^2}{(\gamma+1)M_s^2} \right) \right]^{\frac{1}{2}} \right\} - \left(M_s^2 - \left[\left(\gamma M_s^2 - \frac{\gamma-1}{2} \right) \left(\frac{\gamma-1}{2} M_s^2 + 1 \right) \right]^{\frac{1}{2}} \right) \tag{6}$$

When M_{p2} is greater than 1.0, the projectile is moving supersonically relative to the flow behind the shock wave (or the blast wave) with its Mach number M_s. Meanwhile, when M_{p2} is less than 1.0, the projectile is moving with a subsonic velocity with respect to the flow behind the blast wave. The conditions in which M_{p2} is greater than 1.0 or less than 1.0 are referred to as supersonic and subsonic overtaking conditions, respectively. If the projectile Mach number is less than the blast-wave Mach number ($M_{p1} < M_s$), the projectile cannot overtake the blast wave. This is known as the impossible overtaking condition.

These three conditions are illustrated in Fig. 3, in which the projectile Mach number M_{p1} is plotted against the shock wave Mach number M_s. The solid line indicates the flow state in which $M_{p1} = M_s$, where the projectile just catches up to the moving shock wave. Below this line, overtaking is impossible, as the projectile velocity is less than the shock wave velocity. The dotted line

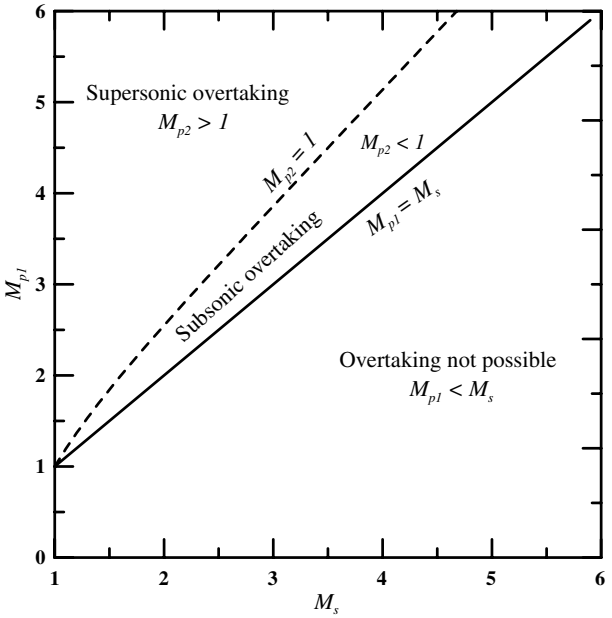

Fig. 3 Flow regimes of moving projectile and blast wave.

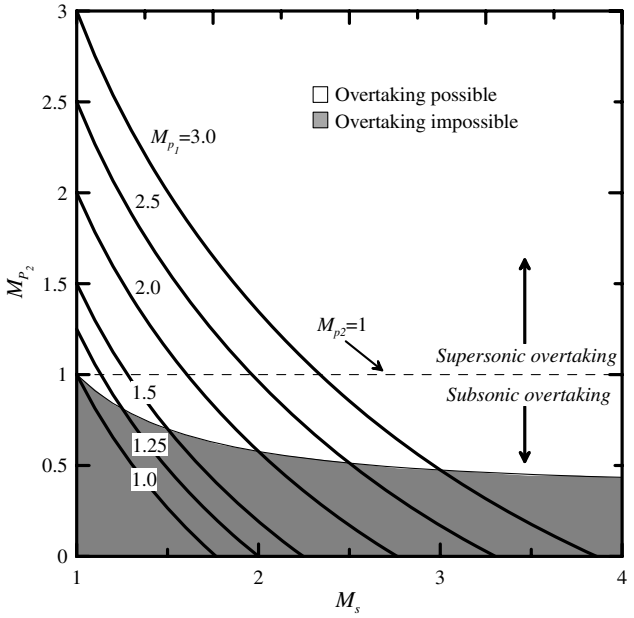

Fig. 4 Overtaking flow regimes based on the relative projectile Mach number.

($M_{p2} = 1$) demarcates the supersonic and subsonic overtaking regimes. In the case of supersonic overtaking, the projectile velocity with respect to the flow behind the shock wave is supersonic, and hence the wave system produced by the motion of the projectile cannot travel upstream of it. In this situation, the shock wave will not be affected by the perturbations produced by the wave system associated with the projectile until the projectile catches up to it. Another important feature of the supersonic overtaking condition is the generation of a bow shock wave ahead of the projectile.

If the relative projectile Mach number with respect to the flow behind the shock wave is less than 1.0, the wave system associated with the projectile can travel upstream and the shock wave will be disturbed before the projectile reaches it. This is referred to as the subsonic overtaking condition, and no bow shock wave is generated ahead of the projectile due to the subsonic motion when it is moving behind the preceding shock wave.

However, in actual flowfields in which the spherical blast wave is expanding, the preceding conditions change dramatically. The overtaking conditions based on the relative projectile Mach number M_{p2} are described in more detail now, to understand how they are related to the actual conditions of a projectile discharged from the launch tube. Figure 4 shows the variation of relative projectile Mach number M_{p2} with respect to the shock wave Mach number M_s for several values of projectile Mach number M_{p1}. The shaded area refers to the flow regime in which the projectile cannot overtake the shock wave, and the boundary of two regimes of possible and impossible overtaking conditions represents the condition $M_s = M_{p1}$, where the projectile just catches up to the shock wave. The dotted line $M_{p2} = 1$ demarcates the subsonic and supersonic overtaking regimes.

Here, it is again noted that the preceding analytical results are obtained based on one-dimensional normal shock relationships, in which the normal shock wave Mach number and the projectile Mach number remain constant. However, in real situations, a blast wave is produced instead of the normal shock wave, as shown in Fig. 1, and attenuates with the propagation distance. For an initial blast wave with a given strength M_s, the blast wave attenuates with propagation along a constant M_{p1} line in the near field of the launch tube, as shown in Fig. 4. This implies that the projectile overtaking criterion cannot be determined using only the initial flow conditions.

In the present study, a computational fluid dynamics method using a moving-grid system was employed to understand the projectile overtaking problems that are applicable to actual conditions. A normal shock wave is assumed at the exit of the launch tube and has its initial Mach number M_s. In computations, the values of M_s and the projectile Mach number M_{p1} are varied to investigate the projectile overtaking phenomena.

III. Computational Methodology

The computational analysis is done using a commercial software CFD-FASTRAN, which makes use of a density-based finite volume method that solves the two-dimensional axisymmetric Euler equations for inviscid flow in the desired domain. The solver uses Van Leer's flux-vector-splitting scheme for spatial discretization, which has a spatial accuracy of first-order. To improve the spatial accuracy, the Osher–Chakravarthy flux limiter is used, which is third-order-accurate in space. The time integration is carried out using a point Jacobi fully implicit scheme.

A. Chimera Mesh

CFD-FASTRAN employs the chimera mesh scheme for structured grids. For simulating the projectile motion, this chimera mesh scheme allows the overlapping of one zone over the other. This method uses a hole-cutting algorithm in which those cells in a particular zone that are overlapped by a wall boundary of another overset zone are blanked and the chimera-boundary cells are identified. In the present computations, a set of multiblock grids around the projectile (minor grids) is constructed and these surrounding grids that are to move typically overlap the background grids (major grids) of the launch tube and near field. Subsequently, a communication between the chimera-boundary cell centroids and the overlapping cell nodes is established through a trilinear interpolation. The required parameters are then calculated in all cells for each time step.

In computations, the projectile is identified as the moving body and is modeled with a motion of 6 degrees of freedom (DOF). The 6-DOF motion requires Euler's equations of motion (6 scalar equations) to be numerically solved at each time step to obtain the displacement and velocities from the force and moments. The physical information required for simulating 6-DOF motion in the present problem are the mass of the projectile, initial center of gravity in the inertial frame of reference, mass moment of inertia in the axis system of the projectile, orientation of the projectile axis system with respect to the inertial frame of reference, constraints on motion, and the aerodynamic forces and moments acting on the projectile, which are obtained by solving the domain numerically. Based on the 6 DOF, the minor grids constructed around the projectile move

through the background grids on the launch tube and near field, communicating the resolved parameters with each other.

B. Computational Domain, Grid System, and Boundary Conditions

Figure 5 illustrates the computational domain, the boundary conditions, and the projectile configuration used in the present study. The projectile has a length of 50 mm and diameter of 20 mm. When the computations start, a moving shock wave is assumed at the exit of the launch tube in which the projectile is kept inside at a distance of 50 mm behind the shock wave. Structured quadrilateral cells were used to discretize the computational domain. To determine the optimum mesh size, a grid independence study was performed for a projectile Mach number of 2.25 and is shown in Fig. 6. It can be seen that except for the first case, in which the number of cells are 55,000, there is not much difference between projectile acceleration histories captured by the other two cases. However, the minimum acceleration is rather higher for the 200,000 cells compared with the 125,000 cells. The number of cells has hence been chosen to be 200,000.

The flows ahead and behind the projectile are assumed to be in the same condition as that of the flow behind the moving shock wave that is at the exit of the launch tube, and the projectile also is moving with the velocity of the flow behind the moving shock when the computation starts. The same flow conditions as that of the flow ahead and behind the projectile are assigned to the rear end of the launch tube as inlet boundary conditions. This is a quite reasonable assumption, as it refers to a condition of the compression explosion in a ballistic range facility [6]. The computations are carried out only up to the point at which the projectile is overtaking the blast wave. During this short duration, the high-pressure tube in which the compression explosion occurs can supply the flow conditions at a constant rate, and no expansion waves from the projectile base reach the rear side of the launch tube.

The initial Mach number M_s of the shock wave that is at the exit of the launch tube is varied (1.4, 2.0, and 2.5) to get various flowfields. The projectile Mach number and the flow conditions behind the shock wave were calculated from one-dimensional normal shock relations for a moving shock wave.

IV. Results and Discussion

A. Validation of the Results

To examine the numerical accuracy of the present computational method, a particular case from [7] is analyzed. The Mach number of the shock wave (M_s) at the exit of the launch tube is 5.0 when the computation starts, and the Mach number of the projectile (M_p) is 4.0. The projectile mass is 50 g. As seen from Fig. 7, the projectile acceleration history agrees very well with that of [7]. Figure 8 shows the comparison of the flowfield of the present computational method with the numerical schlieren of another case ($M_s = 3.0$ and $M_p = 2.2$) in [7]. The locations of projectile, blast wave, and bow shock are matching very well with the numerical schlieren. It is also seen that the contact discontinuities, vortical structures, supersonic jet, Mach disk, and the focusing shock wave behind the projectile are well captured using the present computational method.

B. Analysis of the Results

Figure 9 shows the acceleration history of the projectile having a Mach number M_{p1} equal to 1.75. The Mach number of the shock wave at the launch tube exit (M_s) is 2.5. When the projectile is inside the launch tube, projectile velocity u_p, postshock velocity u_2, and the flow velocity behind the projectile are the same, and hence projectile acceleration is zero. At state a, shown in Figs. 9 and 10, the head of the projectile is coming out of the launch tube and it starts accelerating due to the pressure difference. A secondary shock wave is forming outside the launch tube, as explained in the Introduction, due to the shock wave diffraction at the launch tube exit. A sudden drop in acceleration is observed at state b, as the projectile is interacting with the secondary shock wave.

During this period, the projectile is accelerating slightly from state c to state d when it has passed through the secondary shock wave. It can be seen that after the projectile passed through the secondary shock wave, a bow shock wave is forming in front of the projectile as it travels from a low-velocity flow behind the secondary shock wave to a high-velocity flow behind the PBW. At this period, M_{p2} becomes greater than 1.0, as will be explained later.

At state d, the projectile is on the verge of discharge from the launch tube and experiences a sudden retardation due to the expansion of the gases from the launch tube behind the projectile. From state e onward, the projectile experiences fluctuations in the acceleration due to the effects of a developing underexpanded jet behind it. It can be seen that a Mach disk is forming behind the projectile in the underexpanded jet. This is to adjust the pressure levels of flow just behind the projectile and the flow that is being discharged from the launch tube. During the initial period of the development of the underexpanded jet, unsteady vortical structures can be observed at both the ends of the Mach disk.

At state f, the bow shock wave in front of the projectile catches up to the primary blast wave and there will be a series of expansion waves traveling between the front side of the projectile and the bow shock wave. This is necessary for the bow shock wave to adjust its strength consistent with the relative velocity of the projectile and the gas flow around it. The slight decrease in the deceleration of the

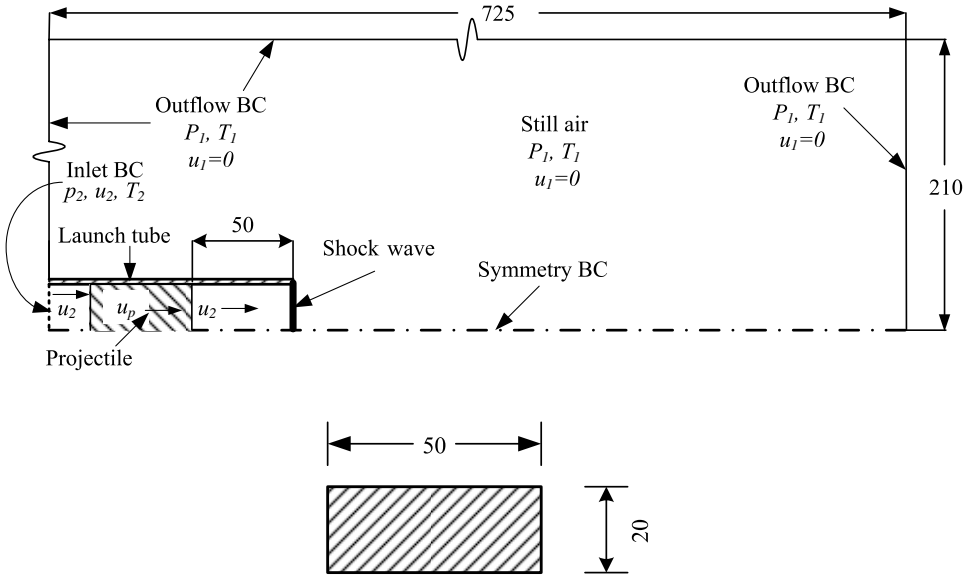

Fig. 5 Computational domain, projectile configuration, and boundary conditions (BC).

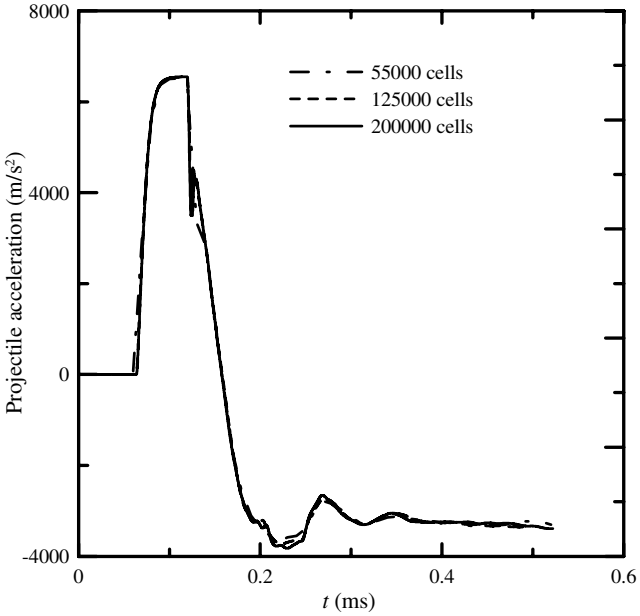

Fig. 6 Variation of projectile acceleration with number of grid cells.

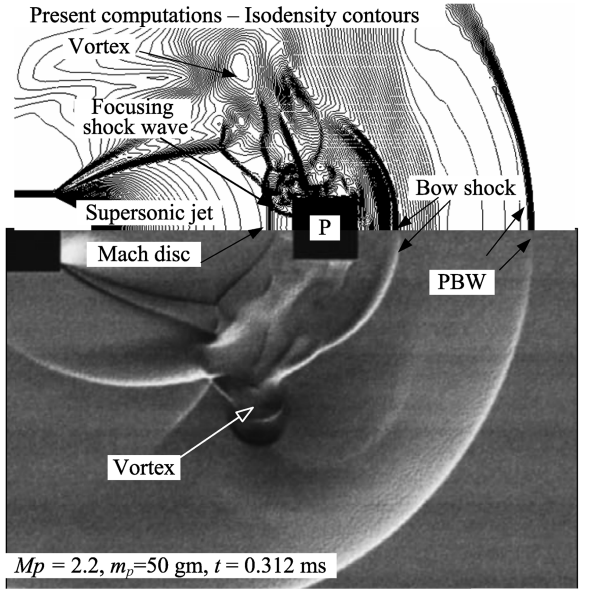

Fig. 8 Comparison of isodensity contours with numerical schlieren (Jiang et al. [7]).

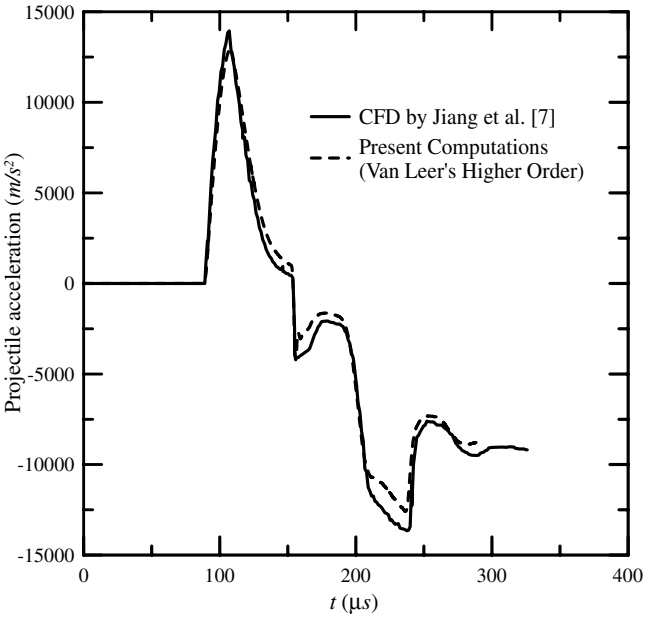

Fig. 7 Comparison of projectile acceleration histories.

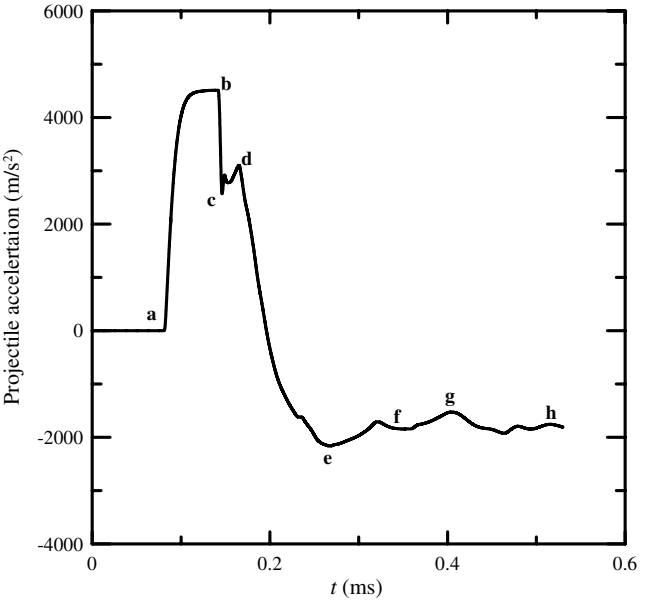

Fig. 9 Acceleration history of a cylindrical projectile ($M_{p1} = 1.75$ and $M_s = 2.5$).

projectile from state f to state g is due to this excursion of the expansion waves between the bow shock and the projectile.

The bow shock has reached the PBW at state g and has now attained a consistent strength when it merges with the PBW, and triple points are formed at each side of the projectile due to the bow-shock/blast-wave interaction. The projectile slightly decelerates due to the increased pressure and density conditions ahead of the projectile for which the flow is stagnant. This completes the overtaking process, as the bow shock wave in front of the projectile is now equivalent to the one that is formed on a supersonic body moving through stagnant air.

Figure 11 shows the isodensity contours of the projectile moving at a Mach number of 1.25. The initial Mach number of the shock wave at the exit of the shock tube is 2.0. Some of the flowfield features are similar to those of the previous case. One notable difference is the absence of the secondary shock wave in the unsteady jet in front of the projectile. This is due to the weaker diffraction the shock wave at the launch tube exit. Another observable difference is in the shear layers formed along the projectile side walls. In Fig. 10, the shear layers are found to be more attached to the projectile walls than in Fig. 11. This is due to the strengths of the bow shock waves produced in each case. In the first case, in which the projectile Mach number is 1.75, the bow shock wave is stronger due to an increased relative velocity of the projectile with respect to the flow behind the blast wave when compared with the case in which the projectile Mach number is 1.25. A weaker shock wave cannot exert more pressure on the shear layers to make them attached to the projectile wall, and hence for a reduced projectile Mach number and the blast-wave strength, the shear layers are found to be more separated from the projectile wall.

The Mach disk formed in the underexpanded jet behind the projectile in this case ($M_{p1} = 1.25$) is found to be smaller than that in the first case, in which $M_{p1} = 1.75$. This can be attributed to the weaker expansion of the gas behind the projectile. However, the size of the Mach disk varies as the projectile moves further away from it. The moving projectile will develop a low-pressure zone just behind it and this will lower the strength of the Mach disk and it becomes smaller. However, when the projectile is moving away, the pressure

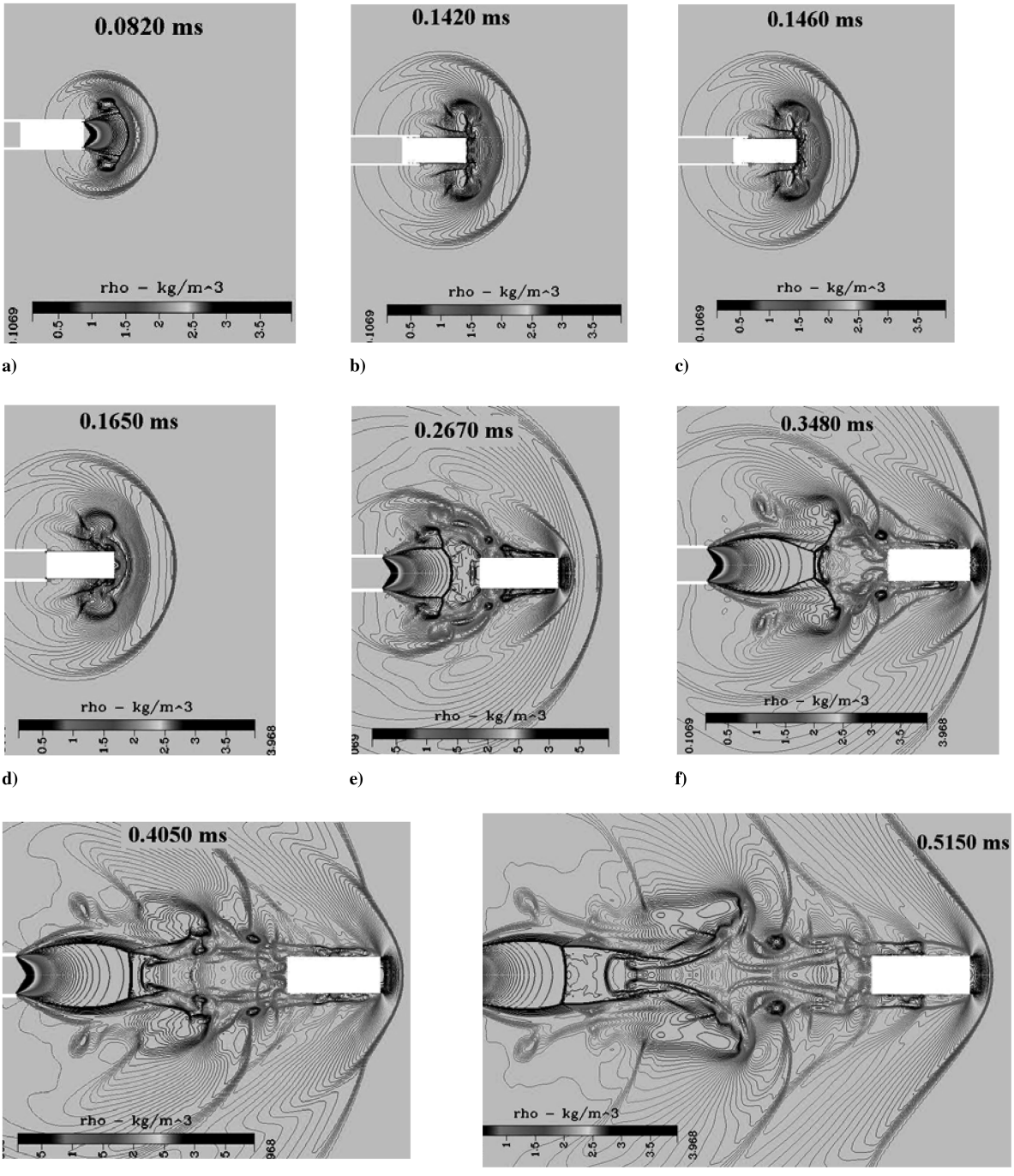

Fig. 10 Isodensity contours corresponding to various time instants in Fig. 9 ($M_{p1} = 1.75$ and $M_s = 2.5$).

is being recovered and the Mach disk starts to grow. This process can be seen through the time frames from $t = 0.367$ to 0.9802 ms in Fig. 11. Also, many shock cells are seen at the end of the launch tube after the underexpanded jet has become steady.

Figure 12 shows the isodensity contours in the flowfield of a projectile with a Mach number of 0.57. The shock wave Mach number M_s is 1.4. Here, the secondary shock wave is also absent in the jet in front of the projectile, due to a weaker expansion. The starting vortices can be clearly seen in front of the projectile. The flowfield exhibits the presence of many vortical structures behind the projectile. It should be noted here that the flow behind the blast wave is completely subsonic. During the diffraction of the shock wave at the exit of the launch tube, expansion waves reenter the launch tube. These expansion waves will make the projectile accelerating even when it is inside the launch tube, as shown in Fig. 13, in which the projectile acceleration histories are plotted for all cases. In the other two cases, in which the flow behind the blast wave is supersonic, the flow will not reenter the launch tube when the shock wave is diffracting at the end of the launch tube. Hence, for these cases, the projectile starts accelerating only when it reaches the exit of the launch tube.

The acceleration history of the projectile with a subsonic Mach number is completely different from that of the supersonic case. The acceleration history fluctuates in a random fashion in this case. This is due to the presence of a number of vortices forming behind the projectile, as seen from Fig. 12. No bow shock wave is forming here and the projectile never overtakes the blast wave, as will be described later.

To investigate the aerodynamic characteristics of the projectile, the drag-coefficient histories of the projectile are plotted for various projectile Mach numbers in Fig. 14. The coefficient of drag of the projectile (C_d) is defined as

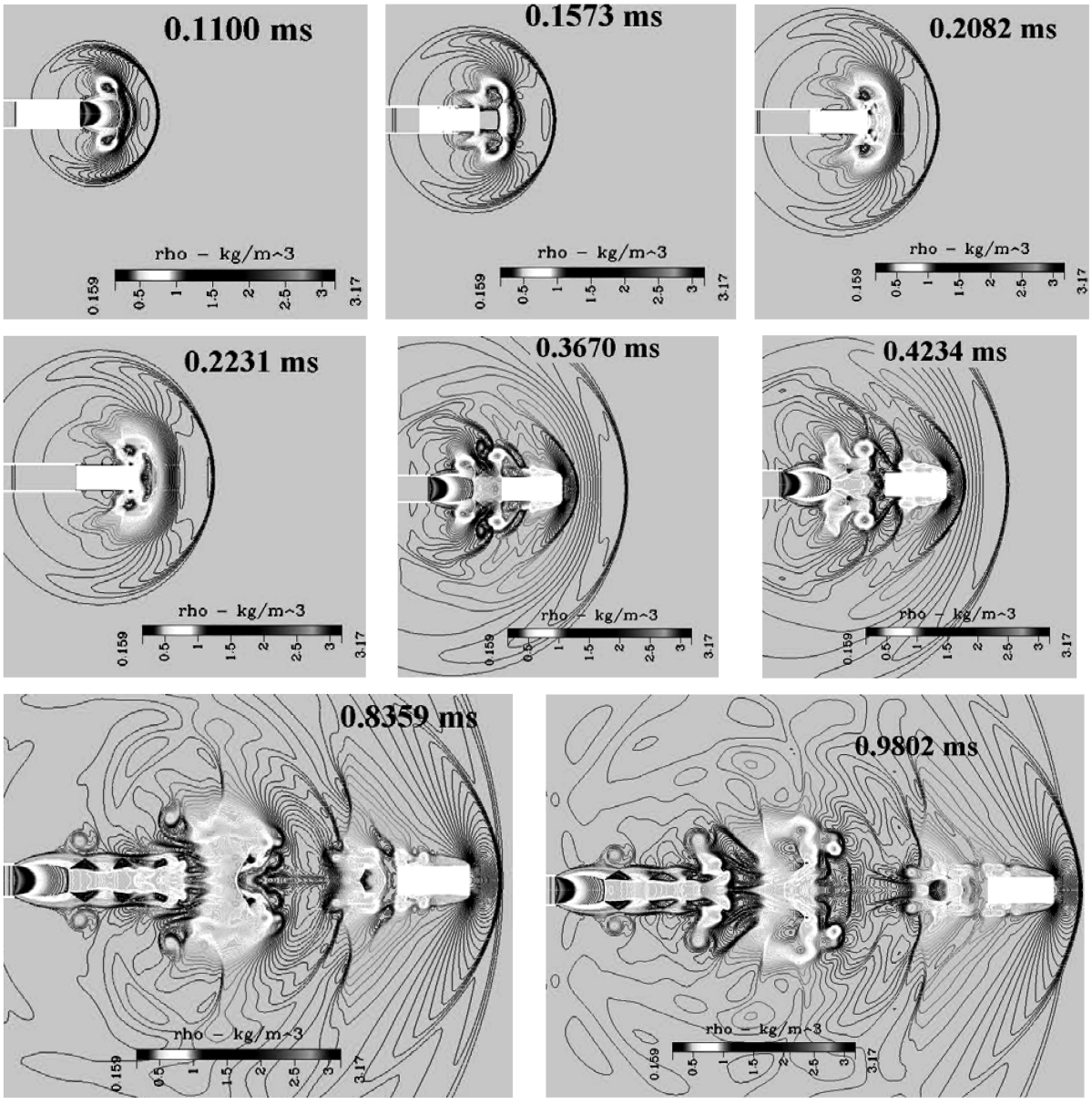

Fig. 11 Isodensity contours $M_{p1} = 1.25$ and $M_s = 2.0$.

$$C_d = \frac{2D}{\gamma p_1 M_{p1}^2 A_p} \tag{7}$$

The same trends as those of the acceleration history can be seen for the C_d curves of the three cases of M_{p1}. It is seen that when the projectile Mach number is decreasing, the peak value of C_d is increasing in the negative direction. Here, it is worth noting that the drag force experienced by the projectile is entirely due to the wave drag and pressure drag, because the present computation uses the inviscid flow assumptions. For reduced projectile Mach numbers, the blast wave is also weak because of the chosen conditions. Hence, for smaller projectile and blast-wave Mach numbers, the strength of the shock system produced around the projectile is weak compared with larger projectile and blast-wave Mach numbers. This will induce less drag force on the projectiles traveling at reduced velocities, and hence the coefficient of drag will increase in the negative direction, giving the projectile a thrust force.

It should also be noted that the drag coefficient in the negative direction is maximum for $M_{p1} = 0.57$, where the projectile has the least Mach number. It should be noted that this happens when the projectile is inside the launch tube. As mentioned early, for the projectile Mach number of 0.57, the flow is completely subsonic and the expansion wave will reenter the launch tube and interact with the projectile, as shown in Fig. 12. This reduces the drag on the projectile due to the pressure difference, and hence the drag coefficient peaks in the negative direction when the projectile is inside the launch tube, as seen from Fig. 14.

To identify the motions of projectile and the blast wave and overtaking points, the x–t diagram is presented in Fig. 15. The blast-wave path starts from the exit of the launch tube, and the projectile starts from a location 50 mm behind the shock wave that is at the exit of the launch tube. The paths for the projectile and the blast wave are converging and coming very close at certain points for the cases of $M_{p1} = 1.75$ and 1.25. These points are identified as the overtaking points. For $M_{p1} = 1.75$ and 1.25, the overtaking points are at 0.34 and 0.835 ms, respectively. It is noted that the blast-wave path and projectile path never meet at a specific point. This is because there will be a single detached shock wave in front of the projectile after the projectile overtakes the blast wave. Hence, the projectile path will be behind the shock wave path by the shock standoff distance, as seen from Fig. 15. The shock standoff distances in the cases of $M_{p1} =$ 1.75 and 1.25 are 15 and 23 mm, respectively. In the case of $M_{p1} = 0.57$, the projectile and blast-wave paths are diverging and the projectile never overtakes the blast wave. Hence, the overtaking point is at infinity for this case, as seen from Fig. 15.

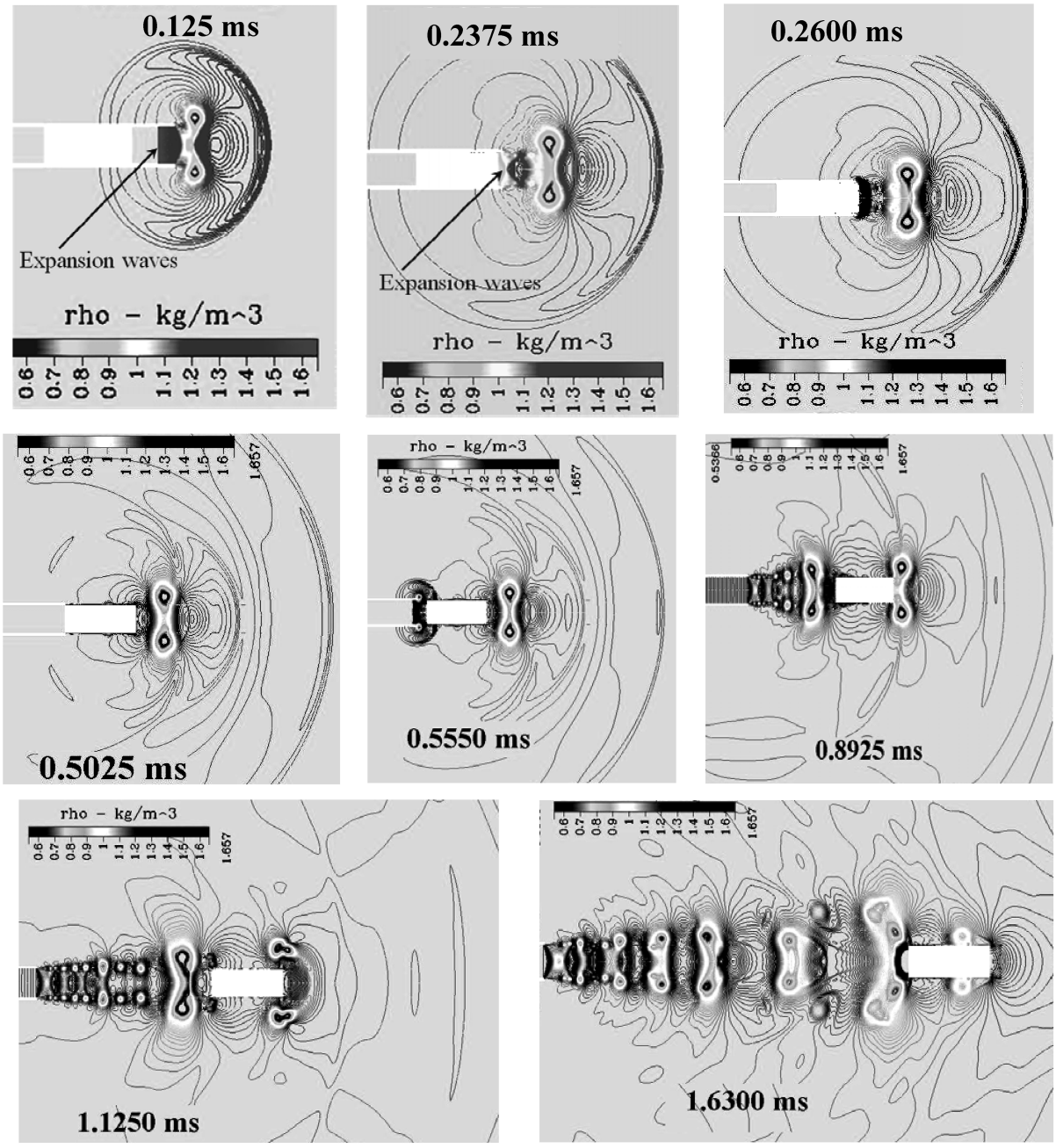

Fig. 12 Isodensity contours $M_{p1} = 0.57$ and $M_s = 1.4$.

The overtaking points should be identified in the projectile drag-coefficient history to understand how the overtaking process affects the projectile aerodynamic characteristics. In Fig. 14, the overtaking points are identified, and it is seen that there are hardly any changes in the drag coefficients at the overtaking points. For the case of $M_{p1} = 1.75$, the overtaking process starts from a constant drag state in which the bow shock catches up to the blast wave, to a slightly increased drag state when the projectile comes out of the blast flowfield. The overtaking process starts as a transient phenomenon due to the excursion of the expansion waves between the projectile front and the bow shock, as described early. This ends up in a steady state after the bow shock is merged with the blast wave and the projectile overtakes it. This leads to the increment in the drag coefficient of the projectile immediately after it overtakes the blast wave.

The increment in the drag of the projectile at the time of overtaking is a strong function of the blast-wave Mach number, as can be seen from the drag history of $M_{p1} = 1.25$. Here, the changes in the drag coefficient are hardly observable, due to a weak blast wave. This is one of the major characteristics of the real flowfield, in which, by the time the projectile overtakes the blast wave, the blast wave will have diminished in its strength and will have a negligible effect on the projectile aerodynamics.

To clarify the effects of the attenuating blast wave on the overtaking process, the variations of the blast-wave Mach number M_s and the relative projectile Mach number M_{p1} with time are shown in Fig. 16 for the computational cases analyzed in the present work. From Fig. 16, it can be seen that during the whole overtaking process, the blast-wave Mach number M_s is varying from an impossible overtaking condition ($M_{p1} < M_s$) to a possible one ($M_{p1} > M_s$) for cases $M_{p1} = 1.75$ and 1.25. For the case of $M_{p1} = 1.75$, the overtaking is impossible until time t_1, as before this time, the projectile Mach number $M_{p1} = 1.75$ is less than the blast-wave Mach number M_s. After the blast wave is diminished enough (after point t_1), the overtaking becomes possible. Hence, in the whole motion of the projectile, the overtaking is impossible for a small time duration. This time duration solely depends on the blast-wave attenuation for a given projectile Mach number M_{p1}. For larger

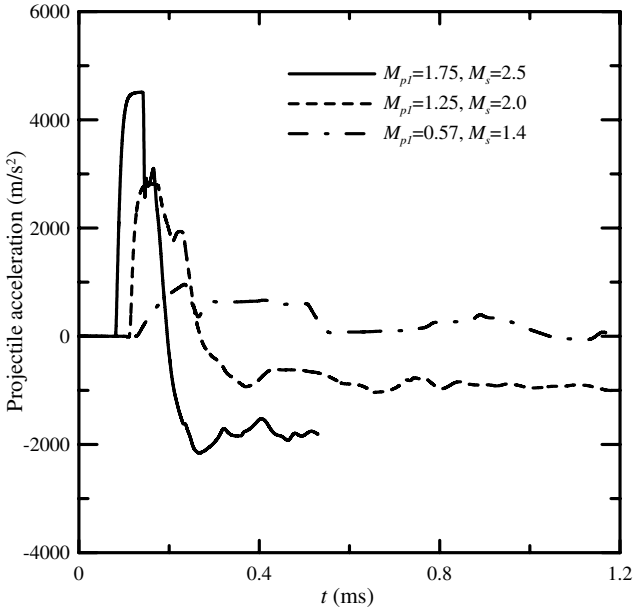

Fig. 13 Acceleration histories of the projectiles for various Mach numbers.

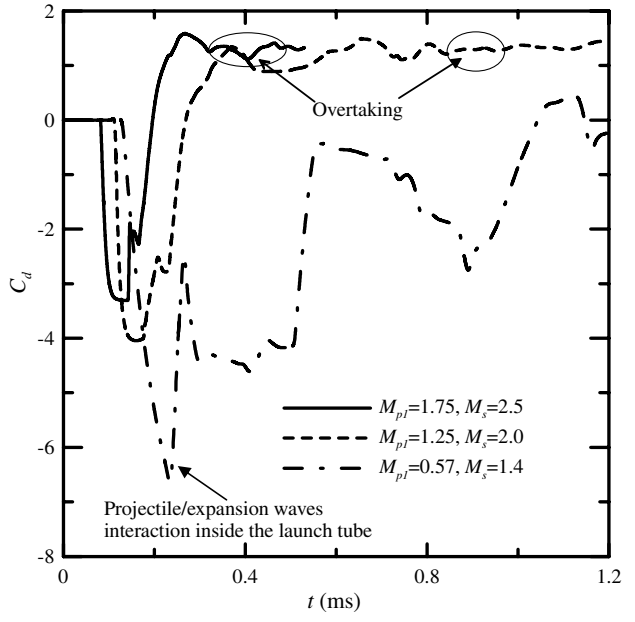

Fig. 14 Drag histories of the projectiles for various Mach numbers.

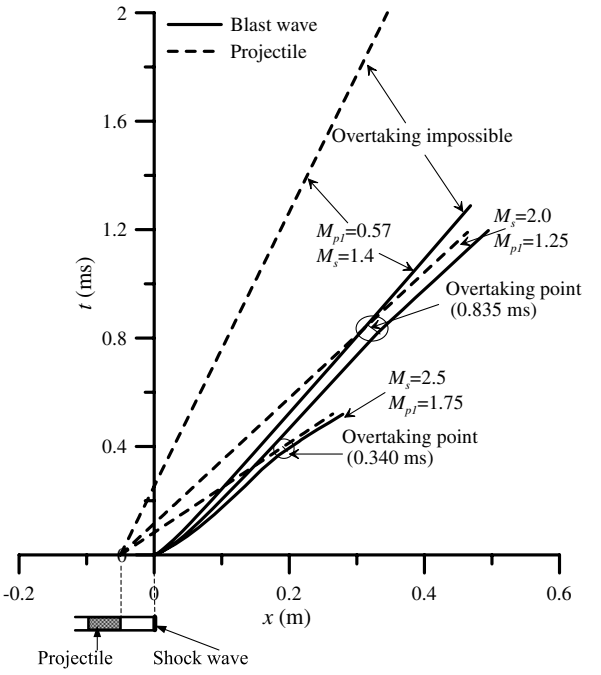

Fig. 15 An *x–t* diagram of the projectiles for various Mach numbers.

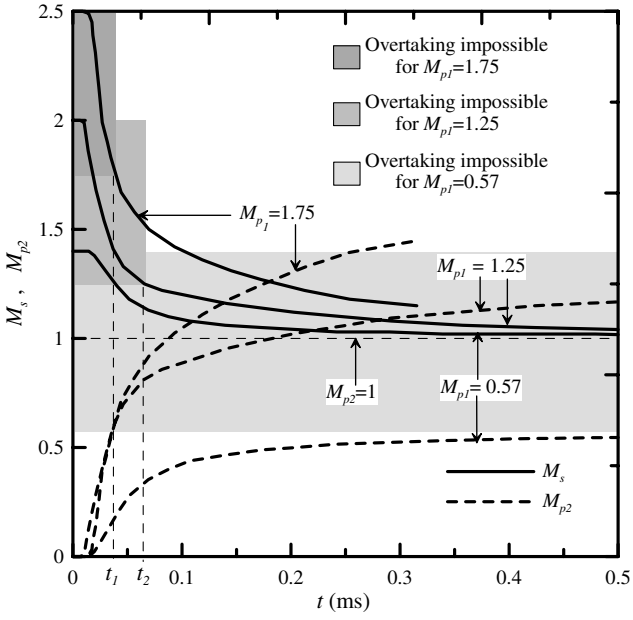

Fig. 16 Variation of M_s and M_{p2} with respect to time.

blast-wave Mach numbers M_s, the impossible overtaking condition lasts for more time for the same projectile Mach number M_{p1}.

For the case of $M_{p1} = 1.25$, the overtaking condition also changes from an impossible one to a possible one. Here, the time duration for the impossible condition (up to t_2) is more than with the first one. Hence, it is impossible to judge based on initial conditions whether the projectile overtakes the blast wave in real flow situations, as the projectile always passes through an impossible overtaking condition during the initial period of its motion. However, for $M_{p1} = 0.57$, the overtaking condition is always in the impossible regime and the projectile never overtakes the blast wave.

The subsonic and supersonic overtaking regimes of the projectile can be identified from the variation of the relative projectile Mach number M_{p2} in Fig. 16. For both $M_{p1} = 1.75$ and 1.25, the relative projectile Mach number M_{p2} varies from a value less than 1 in the earlier part of projectile motion to greater than 1 in the later part in which the blast wave has diminished. This makes the distinction of the flowfields almost impossible based on M_{p2}, as determined by Watanabe et al. [13]. Using the one-dimensional theory, they showed that the flowfields can be distinguished solely based on the relative projectile Mach number M_{p2}. Because they assumed constant blast-wave strength, the relative projectile Mach number also was constant and subsonic or supersonic overtaking conditions could be computationally created. However, in the real situations, as the present computations show, the projectile will pass through a mixed situation of both subsonic and supersonic flow regimes during its travel to overtake the blast wave. It will always have a subsonic motion relative to the flow behind the blast wave for a very small duration during its initial periods of motion, and it becomes a supersonic motion later when the blast wave has diminished in its strength. Thus, the subsonic overtaking regime of the projectile in the actual flow problems is a purely transient phenomenon.

In such a situation, the projectile cannot have a mere subsonic overtaking condition as illustrated in the previous work [13], unless the distance between the projectile and shock wave that is diffracting

at the exit of the launch tube is very small. However, it should be noted from Fig. 16 that for smaller initial Mach numbers of the diffracting shock wave, there can be a longer subsonic overtaking region, indicating the chance of a subsonic overtaking. Thus, there does exist a chance of a subsonic overtaking condition, depending on both the distance between the diffracting shock wave and the projectile when it is inside the tube and the Mach number of the diffracting shock wave. Both of these factors are decided by the gas-expansion process behind the projectile in real gas gun problems. A larger distance between the projectile and the diffracting shock wave implies reduced projectile velocities inside the launch tube, leading to a smaller Mach number of the diffracting shock wave. In this case, even though there will be a longer subsonic overtaking regime, as explained early, the overtaking is less likely to occur because the distance between the projectile and blast wave is greater. Moreover, even if the projectile overtakes the blast wave during this period, the overtaking effect on the projectile aerodynamic characteristics will be negligible, due to the reduced Mach number of the diffracting shock wave and the blast-wave attenuation in a longer subsonic regime. On the other hand, if the Mach number of the diffracting shock wave is high, the subsonic overtaking regime occurs for a very small time duration and the subsonic overtaking is again less likely to be possible. It can hence be inferred that the overtaking process, which may have an influence over the projectile aerodynamic characteristics, will always be supersonic.

It has also been shown in the previous work [13] that the main characteristic of the supersonic overtaking ($M_{p2} > 1$) is a bow shock. However, in the actual flowfields, a bow shock will be produced in a later part of the projectile motion, when the subsonic overtaking condition changes to a supersonic overtaking condition. This can be seen through the projectile flowfields depicted in Figs. 10 and 11. Thus, it is hardly possible to confirm whether the overtaking is supersonic or subsonic based on either the relative projectile Mach number M_{p2} or the presence of the bow shock wave in front of the projectile, such as the one-dimensional studies can do. For the case of $M_{p1} = 0.57$, M_{p2} always lies in the subsonic regime. This does not have any meaning, as in this case, the projectile never overtakes the blast wave.

Though the instantaneous local flowfields on the projectile depend on the relative projectile Mach number M_{p2}, this Mach number cannot be depended upon for studying the projectile aerodynamic characteristics. The projectile passes through transient flow structures and thereby experiences variations in relative projectile Mach number. These transient flow structures are mainly responsible for the drag fluctuations on the projectile rather than for the overtaking process. The drag-coefficient history confirms that the overtaking process makes little difference in the projectile aerodynamic characteristics. This is because in the real flowfield, by the time the projectile overtakes the blast wave, the latter becomes weak and will no longer be able to influence the projectile aerodynamics characteristics to a great extent. However, it should be noted that for very large projectile and blast-wave Mach numbers, the projectile overtakes the blast wave within a very short time and may be influenced greatly by the overtaking process, as the blast waves do not diminish significantly within this time period.

V. Conclusions

A computational study was performed using a moving-grid method to analyze the effects of the projectile overtaking a moving shock wave on the projectile aerodynamic characteristics. A one-dimensional analysis was also carried out to identify the projectile overtaking criteria. The analytical results show that the projectile overtaking flowfields can be in a subsonic or supersonic flow regime, based on the relative projectile Mach number. However, it is found in the present computations that the actual flowfields cannot be distinguished with the relative projectile Mach number only, because the blast-wave strength is diminishing with time and space. It is also noticed that the projectile always passes through a subsonic flow regime relative to the flow behind the blast wave before it overtakes the blast wave. This subsonic overtaking process is a transient phenomenon, and the overtaking process of the projectile, which may have influence over the projectile aerodynamic characteristics, will eventually be supersonic.

The aerodynamic characteristics of the projectile are hardly affected by the overtaking process for smaller blast-wave Mach numbers, as the blast wave will become weak by the time it is overtaken by the projectile. The projectile drag coefficient is more greatly affected by the unsteady flow structures through which the projectile travels in the near field than by the overtaking process. However, for larger projectile and blast-wave Mach numbers, the overtaking effects may be predominant because the projectile overtakes the blast wave within a very short time after it is discharged from the launch tube and the overtaking process involves transient effects of shock interactions.

References

[1] Kim, H. D., and Setoguchi, T., "Study of the Discharge of Weak Shocks from an Open End of a Duct," *Journal of Sound and Vibration*, Vol. 226, No. 5, Oct. 1999, pp. 1011–1028. doi:10.1006/jsvi.1999.2376

[2] Kim, H. D., Lee, D. H., and Setoguchi, T., "Study of the Impulse Wave Discharged from the Exit of a Right-Angle Pipe Bend," *Journal of Sound and Vibration*, Vol. 259, No. 5, Jan. 2003, pp. 1147–1161. doi:10.1006/jsvi.2002.5190

[3] Bagabir, A., and Drikakis, D., "Numerical Experiments Using High-Resolution Schemes for Unsteady, Inviscid, Compressible Flows," *Computer Methods in Applied Mechanics and Engineering*, Vol. 193, Nos. 42–44, Oct. 2004, pp. 4675–4705. doi:10.1016/j.cma.2004.03.012

[4] Sun, M., and Takayama, K., "The Formation of a Secondary Shock Wave behind a Shock Wave Diffracting at a Convex Corner," *Shock Waves*, Vol. 7, No. 5, Oct. 1997, pp. 287–295. doi:10.1007/s001930050083

[5] Sun, M., Siato, T., Takayama, K., and Tanno, H., "Unsteady Drag on a Sphere by Shock Loading," *Shock Waves*, Vol. 14, Nos. 1–2, June 2005, pp. 3–9. doi:10.1007/s00193-004-0235-4

[6] Rajesh, G., Kim, H. D., Setoguchi, T., and Raghunathan, S., "Performance Analysis and Enhancement of the Ballistic Range," *Proceedings of the Institution of Mechanical Engineers, Part G (Journal of Aerospace Engineering)*, Vol. 221, No. 5, 2007, pp. 649–659. doi:10.1243/09544100JAERO229

[7] Jiang, Z., Takayama, K., and Skews, B. W., "Numerical Study on Blast Flow Fields Induced by Supersonic Projectiles Discharged from Shock Tubes," *Physics of Fluids*, Vol. 10, No. 1, 1998, pp. 277–288. doi:10.1063/1.869566

[8] Shapiro, A. H., *The Dynamics and Thermodynamics of Compressible Fluid Flow*, Vol. 1, Ronald Press, New York, 1953, pp. 383–384.

[9] Rajesh, G., Kim, H. D., Matsuo, S., and Setoguchi, T., "A Study of the Unsteady Projectile Aerodynamics Using a Moving Coordinate Method," *Proceedings of the Institution of Mechanical Engineers, Part G (Journal of Aerospace Engineering)*, Vol. 221, No. 5, 2007, pp. 691–706. doi:10.1243/09544100JAERO227

[10] Schmidt, E. M., Fansler, K. S., and Shear, D. P., "Trajectory Perturbations of Fin-Stabilized Projectile Due to Muzzle Blast," *Journal of Spacecraft and Rockets*, Vol. 14, No. 6, 1977, pp. 339–347. doi:10.2514/3.57206

[11] Schmidt, E. M., and Shear, D. P., "Optical Measurements of Muzzle Blast," *AIAA Journal*, Vol. 13, No. 8, 1975, pp. 1086–1091. doi:10.2514/3.60506

[12] Ofengeim, D. K., and Drikakis, D., "Simulation of Blast Wave Propagation over a Cylinder," *Shock Waves*, Vol. 7, No. 5, 1997, pp. 305–317. doi:10.1007/s001930050085

[13] Watanabe, R., Fujii, K., and Higashino, F., "Numerical Solutions of the Flow Around a Projectile Passing Through a Shock Wave," AIAA Paper 95-1790, 1995.

[14] Ahmadikia, H., and Shirani, E., "Transonic and Supersonic Overtaking of a Projectile Preceding a Shock Wave," International Centre for Theoretical Physics, Rept. IC/2001/48, Trieste, Italy, 2001.

M. Costello
Associate Editor